NTNU
Kunnskap for en bedre verden

DEPARTMENT OF MATHEMATICAL SCIENCES

TMA4212 - NUMERICAL SOLUTION OF DIFFERENTIAL EQUATIONS BY DIFFERENCE METHODS

Project 2
A Study of Applications of FEMs on Non-Smooth Solutions

Authors:
Karianne Strand Bergem, Kristin Fullu, Marius Bjerke Stjernstedt

07.04.2024

Table of Contents

List of Figures

List of Tables

0   Abstract

In this project we develop and implement finite element methods (FEMs) for elliptic problems in 1D. We perform analysis of the method, as well as theoretical error analysis. Finally, we implement the method numerically and test it with a known function, before modifying it for special cases.

1   Introduction

We will consider a PDE for modeling a 1D stationary convection diffusion problem on the unit interval. We will introduce the problem and perform analysis of coercivity, continuity, Cea´s lemma, convergence, and through this derive a error bound in H^1. Further we will implement a finite element method (FEM) and show examples with both smooth and non-smooth solutions.

2   Theory

Our model is a boundary problem for a Poission like equation for a convective and diffusive substance, given by

$$-\partial_x(\alpha(x)\partial_x u) + \partial_x(b(x)u) + c(x)u = f(x) \quad \text{in} \quad \Omega = (0,1) \tag{1}$$

where u is the concentration of the substance, $\alpha(x) > 0$ is the diffusion coefficient, $b(x)$ is the convective/fluid velocity, $c(x)$ is the decay rate of the substance, and $f(x)$ is a source term. We want to study whether there exists a solution to this problem. To do this, we wish to apply the Lax-Milgram theorem, which states that the variational problem

$$a(u,v) = F(v) \quad \forall \; v \in H_0^1(0,1). \tag{2}$$

admits a unique solution $u \in H_0^1(0,1)$ if "F is a continuous linear functional, and that a is a continuous, coercive bilinear form" [1](p. 15). We aim to show that the requirements hold in our case.

2.1   Problem Formulation

First, we need to rewrite our problem on a form that fits Lax-Milgram. We therefore define $F(v) := \int_0^1 f(x)v \; dx$, and thus

$$a(u,v) = \int_0^1 (-\partial_x(\alpha(x)\partial_x u) + \partial_x(b(x)u) + c(x)u)v \; dx.$$

Now, we apply integration by parts to the first and second term, leaving us with

$$\left([-\alpha(x)\partial_x uv]_0^1 - \int_0^1 -\alpha(x)\partial_x uv' \; dx \right) + \left([b(x)uv]_0^1 - \int_0^1 b(x)uv' \; dx \right) + \int_0^1 c(x)uv \; dx.$$

Since $v \in H_0^1(0,1)$, $v(0) = 0 = v(1)$, then the first and third term becomes zero, and we are left with

$$a(u,v) = \int_0^1 \alpha(x)u_x v_x - b(x)uv_x + c(x)uv \; dx = \int_0^1 f(x)v \; dx = F(v), \tag{3}$$

---

which is a weak formulation of (1).

2.2   Bilinearity and Continuity

Next, we can show that $a(u, v)$ is a bilinear and continuous form on $H^1 \times H^1$. To do this, we show linearity in the first and second argument. In the first argument:

$$a(\lambda u + w, v) = \int_0^1 \alpha(x)(\lambda u + w)_x v_x - b(x)(\lambda u + w)v_x + c(x)(\lambda u + w)v \, dx$$

$$= \lambda \int_0^1 \alpha(x)u_x v_x - b(x)uv_x + c(x)uv \, dx + \int_0^1 \alpha(x)w_x v_x - b(x)wv_x + c(x)wv \, dx = \lambda a(u, v) + a(w, v)$$

Thus, we have proved that $a(u, v)$ is linear in the first argument. By doing a similar computation in the second argument, it shows that $a(u, v)$ is linear in the second argument as well, and thus it is bilinear.

To show continuity, we must show that

$$a(u, v) \leq M \|u\|_{H^1} \|v\|_{H^1},$$

where

$$\|u\|_{H^1}^2 = \int_0^1 u^2 \, dx + \int_0^1 u_x^2 \, dx = \|u\|_{L^2}^2 + \|u_x\|_{L^2}^2. \tag{4}$$

Using the triangle inequality and Cauchy-Schwarz, we can write

$$a(u, v) \leq \|a\|_{L^\infty} \left| \left(\int_0^1 u_x^2 \, dx \right)^{1/2} \cdot \left(\int_0^1 v_x^2 \, dx \right)^{1/2} \right| + \|b\|_{L^\infty} \left| \left(\int_0^1 u^2 \, dx \right)^{1/2} \cdot \left(\int_0^1 v_x^2 \, dx \right)^{1/2} \right|$$

$$+ \|c\|_{L^\infty} \left| \left(\int_0^1 u^2 \, dx \right)^{1/2} \cdot \left(\int_0^1 v^2 \, dx \right)^{1/2} \right|.$$

Observing the terms as being L^2-norms, we write

$$a(u, v) \leq \|a\|_{L^\infty} \|u_x\|_{L^2} \cdot \|v_x\|_{L^2} + \|b\|_{L^\infty} \|u\|_{L^2} \cdot \|v_x\|_{L^2} + \|c\|_{L^\infty} \|u\|_{L^2} \cdot \|v\|_{L^2}$$

Using (4), we can rewrite this as

$$a(u, v) \leq (\|a\|_{L^\infty} + \|b\|_{L^\infty} + \|c\|_{L^\infty}) \|u\|_{H^1} \cdot \|v\|_{H^1}.$$

Thus we have shown that $a(u, v)$ is continuous with $M = (\|a\|_{L^\infty} + \|b\|_{L^\infty} + \|c\|_{L^\infty})$. Then, we can show that $F(v)$ is a linear continuous (bounded) functional on H^1. We have that

$$\|b\|_{L^\infty} + \|f\|_{L^2} < \infty \Rightarrow \|f\|_{L^2} < \infty.$$

We also have

$$\|F\|_{(H^1)'} = \sup_{1 \leq i \leq N} \frac{|F(v)|}{\|v\|_{H^1}} < \infty. \quad [1] \tag{5}$$

Then,

$$|F(v)| = \left| \int_0^1 f(x)v(x) \, dx \right| \leq \left| \left(\int_0^1 f(x)^2 \, dx \right)^{1/2} \left(\int_0^1 v(x)^2 \right)^{1/2} \right| = \|f\|_{L^2} \|v\|_{L^2}.$$

Thus, we can rewrite (5) as

$$\|F\|_{(H^1)'} = \sup_{1 \leq i \leq N} \frac{\|f\|_{L^2} \|v\|_{L^2}}{\|v\|_{H^1}} < \sup_{1 \leq i \leq N} \|f\|_{L^2} < \infty.$$

We have then shown that $F(v)$ is bounded on H^1.

2.3   Coercivity

We now show that $a(u,v)$ is coercive, and to do this we begin with showing that it satisfies a given Gårding inequality:

$$a(u,u) \geq (\alpha_0 - \frac{\varepsilon}{2}\|b\|_{L^\infty}) \int_0^1 u_x^2 \, dx + (c_0 - \frac{1}{2\varepsilon}\|b\|_{L^\infty}) \int_0^1 u^2 \, dx \quad \text{for all} \quad \varepsilon > 0, \qquad (6)$$

where $\alpha_0 = \min_{x \in [0,1]} \alpha(x)$ and $c_0 = \min_{x \in [0,1]} c(x)$. First, we have the expression

$$a(u,u) = \int_0^1 \alpha(x)u_x^2 - b(x)uu_x + c(x)u^2 \, dx. \qquad (7)$$

Next, we use that

$$-\int_0^1 b(x)uu_x \, dx \geq -\|b\|_{L^\infty} \int_0^1 uu_x \, dx \geq -\|b\|_{L^\infty} \left(\frac{1}{2\varepsilon} \int_0^1 u^2 \, dx + \frac{\varepsilon}{2} \int_0^1 u_x^2 \, dx \right)$$

obtained using Youngs inequality from the project description. We use this to conclude that

$$a(u,u) \geq \alpha_0 \int_0^1 u_x^2 \, dx + c_0 \int_0^1 u^2 \, dx - \frac{\varepsilon}{2}\|b\|_{L^\infty} \int_0^1 u_x^2 \, dx - \frac{1}{2\varepsilon}\|b\|_{L^\infty} \int_0^1 u^2 \, dx,$$

which we can rewrite into (6). Now, we can use the Gårding inequality to prove that $a(u,v)$ is coercive when $\|b\|_{L^\infty} < \sqrt{2\alpha_0 c_0} = \sqrt{5}$. To show coercivity, we must show that $a(u,u) \geq \lambda\|u\|_{H^1}^2 \forall u \in H^1$, for some $\lambda \geq 0$. To do this, we look at (6). If we manage to find some ε such that $(\alpha_0 - \frac{\varepsilon}{2}\|b\|_{L^\infty}) = (c_0 - \frac{1}{2\varepsilon}\|b\|_{L^\infty})$, we can rewrite (6) with (4) and some obtained constant λ. We perform the computation as follows:

$$(\frac{1}{2} - \frac{\varepsilon}{2}\sqrt{5}) = (5 - \frac{1}{2\varepsilon}\sqrt{5}).$$

Solving for ε:

$$\varepsilon^2 + \frac{9}{\sqrt{5}}\varepsilon - 1 = 0 \Rightarrow \varepsilon = \frac{\sqrt{505} - 9\sqrt{5}}{10}.$$

We have thus shown that with this particular ε, if

$$\|b\|_{L^\infty} < \sqrt{5},$$

then $a(u,v)$ is coercive with

$$\lambda = \frac{11 - \sqrt{101}}{4}.$$

2.4 Existence of Solution

As all the requirements stated by the Lax-Milgram theorem has been fulfilled, then we can conclude that (2) admits a unique solution, $u \in H_0^1(0,1)$.

2.5 Error Bound

Now, we consider the $\mathbb{P}_1$ FEM (V_h) problem,

$$(V_h) \quad \text{Find } u \in V_h \text{ such that} \quad a(u_h, v_h) = F(v_h) \quad \forall \ v_h \in V_h \tag{8}$$

where $V_h = X_h^1(0,1) \cap H_0^1(0,1)$. We want to obtain an error bound to better evaluate a potential numerical solution of this problem. To do this, we need to show that Cea's lemma holds, before combining this result with an interpolation error estimate.

To prove that Cea's lemma holds, we must first show Galerkin orthogonality for this problem. That is, if u and u_h are the solutions of the infinite and finite dimensional problems respectively, then

$$a(u - u_h, v_h) = 0 \quad \forall \ v \in V_h. \tag{9}$$

We can use that a is bilinear to show that

$$a(u - u_h, v_h) = a(u, v_h) - a(u_h, v_h) = F(v_h) - F(v_h) = 0.$$

Thus we have shown Galerkin ortogonality for the $\mathbb{P}_1$ FEM (V_h). We can now proceed to show that Cea's Lemma holds for this problem. That is,

$$\|u - u_h\|_v^2 \leq \frac{M}{\lambda} \|u - u_h\|_V, \quad v_h \in V_h. \tag{10}$$

Due to coercivity, we can write

$$\lambda \|u - u_h\|_{H^1}^2 \leq a(u - u_h, u - u_h).$$

Further, we expand the second term in a with v_h:

$$\lambda \|u - u_h\|_{H^1}^2 \leq a(u - u_h, u - v_h + v_h - u_h).$$

Since a is bilinear, we can write

$$\lambda \|u - u_h\|_{H^1}^2 \leq a(u - u_h, u - v_h) + a(u - u_h, v_h - u_h).$$

Further, we have that $v_h - u_h \in V_h$. Due to Galerkin orthogonality, we have that $a(u - u_h, v_h - u_h) = 0$. Since a is continuous, we have that

$$\lambda \|u - u_h\|_{H^1}^2 \leq a(u - u_h, u - v_h) \leq M \cdot \|u - u_h\|_{H^1} \cdot \|u - v_h\|_{H^1}.$$

Then

$$\|u - u_h\|_{H^1} \leq \frac{M}{\lambda} \|u - v_h\|_{H^1}.$$

Thus we have shown that Cea´s lemma holds for this problem. We now want to find an H^1 error bound. Assuming that for $u \in H^2$, and using the interpolation error estimate given by [2](p. 5)

$$\inf_{v_h \in X_h^1} \|u - v_h\|_{H^1} \le Kh\|u_{xx}\|_{L^2}, \tag{11}$$

gets us the following error bound on H^1,

$$\|e\|_{H^1} \le Ch\|u_{xx}\|_{L^2}, \quad C = \frac{MK}{\lambda}. \tag{12}$$

3   Numerical Experiments

We now want to solve the $\mathbb{P}_1$ FEM (V_h), (8). We let $\alpha, c \ge 0$ and b be nonzero constants, $\alpha = 1$, $b = 2$, and $c = 5$.

3.1   Implementation of the Method

To solve the problem (V_h), we need to solve a linear system on the form $AU = F$, where A is a stiffness matrix and F is a load vector. We define A and F as

$$A_{ij} = \sum_{K_i \in \tau_h} \int_{K_i} (\alpha \phi_j' \phi_i' - b\phi_j \phi_i' + c\phi_j \phi_i)dx, \quad F_j = \int_0^1 \phi_j f(x)dx,$$

where τ_h is the set of all subintervals $K_i = [x_{i-1}, x_i]$, and ϕ, the FEM basis function, and its derivative is on the form

$$\phi_i(x) = \begin{cases} \frac{x - x_{i-1}}{h_i}, & x \in [x_{i-1}, x_i] \\ \frac{x_{i+1} - x}{h_{i+1}}, & x \in [x_i, x_{i+1}] \\ 0, & \text{otherwise,} \end{cases} \quad \phi_i'(x) = \begin{cases} \frac{1}{h_i}, & x \in [x_{i-1}, x_i] \\ -\frac{1}{h_{i+1}}, & x \in [x_i, x_{i+1}] \\ 0, & \text{otherwise.} \end{cases} \tag{13}$$

To assemble these numerically, we observe that they can be divided into smaller overlapping elements, defined as

$$A_i = \frac{\alpha}{h_i} \begin{bmatrix} 1 & -1 \\ -1 & 1 \end{bmatrix} + \frac{b}{2} \begin{bmatrix} -1 & 1 \\ -1 & 1 \end{bmatrix} + \frac{ch_i}{6} \begin{bmatrix} 2 & 1 \\ 1 & 2 \end{bmatrix}, \quad F_i = \frac{h_i}{2} \begin{bmatrix} f(x_{i-1}) \\ f(x_i) \end{bmatrix}. \tag{14}$$

3.2   Convergence of the Method

To test our method, we introduce a problem with the known solution

$$u_1(x) = x(1 - x), \tag{15}$$

and compute the right hand side by inserting (15) into (1) and obtain

$$f(x) = -5x^2 + x + 4.$$

Using the same parameters α, b and c as previously stated, we build the problem as described in Section 4.1, and solve the linear system gradually refining the grid to analyze the convergence of the method. Doing this, we obtain the rates presented in figure 1. For the H^1 norm, this result is consistent with an error bound computed using (12) with i.e. $C = 1$.

3.3 Reduced Order for Non-smooth Solutions

Until now, we have only worked with smooth solutions. We now shift our focus to non-smooth manufactured solutions on the $(0,1)$ interval, and use two examples defined by

$$w_1(x) = \begin{cases} \frac{x}{\frac{\sqrt{2}}{2}}, & x \in [0, \frac{\sqrt{2}}{2}], \\ \frac{1-x}{1-\frac{\sqrt{2}}{2}}, & x \in (\frac{\sqrt{2}}{2}, 1], \end{cases} \quad \text{and} \quad w_2(x) = x - x^{\frac{3}{4}}, \tag{16}$$

with their respective weak derivatives

$$w_1'(x) = \begin{cases} \frac{\sqrt{2}}{2}, & x \in [0, \frac{\sqrt{2}}{2}], \\ \frac{1}{\frac{\sqrt{2}}{2}-1}, & x \in (\frac{\sqrt{2}}{2}, 1], \end{cases} \quad \text{and} \quad w_2'(x) = 1 - \frac{3}{4}x^{-\frac{1}{4}}.$$

Both w_1 and w_2 are continuous. However, w_1' is not continuous at $x = \frac{\sqrt{2}}{2}$, and w_1' is not continuous at $x = 0$. That is, w_1 and w_2 are not differentiable at $x = \frac{\sqrt{2}}{2}$ and $x = 0$ respectively.

In order to compute a right hand side to solve (8), we originally inserted the exact solutions into (1). However, this is only possible if the inserted $u(x)$ has a second derivative. To proceed, we must therefore check if $w_1(x)$ and $w_2(x)$ belong to the space $H^2(0,1)$. We observe that $w_1 \in L^2(0,1)$ and $w_1' \in L^2(0,1)$. However, we observe that since w_1' is discontinuous, the function is in fact a Heaviside step function. This also means that the Dirac delta function is its weak second derivative. As the Dirac delta function is not in $L^2(0,1)$ [1](p. 14), $w_1 \notin H^2(0,1)$.

Similarly, we observe that $w_2 \in L^2(0,1)$ and $w_2' \in L^2(0,1)$, with the weak second derivative

$$w_2''(x) = \frac{3}{16}x^{-\frac{5}{4}}.$$

The L^2-norm of w_2'' will not converge, meaning $w_2'' \notin L^2(0,1)$. Thus, both w_1 and w_2 belong to $H^1(0,1)$, but not to $H^2(0,1)$. This tells us that we must find an alternative approach to compute the right hand side of the problem.

A good alternative is to use weak formulation of the original problem written in equation (3). Utilising this formulation with the basis functions ϕ_i inserted for v, we can derive a weak form for the right hand side for both non-smooth solutions, giving us an equal overlapping structure as in 3.1 on the form

$$F_k = \frac{h_i}{2} \begin{bmatrix} \int_{K_i} f(x)\phi_{i-1}dx \\ \int_{K_i} f(x)\phi_i dx \end{bmatrix}. \tag{17}$$

Since both w_1, w_2, and their derivatives are defined, we can together with the basis functions use this to construct the new load vector F by writing

$$F(v) = \int_{K_i} f(x)\phi_i dx = \int_{K_i} \alpha w_x \partial_x \phi_i - bw\partial_x\phi_i + cw\phi_i \ dx.$$

In the implementation we make sure to include the point $x = \frac{\sqrt{2}}{2}$ in our list of x-values to compensate for the discontinuity for w_1' at this value.

As one can see in figure 2 and 3, the convergence for both solutions are outliers from what is expected as convergence rates for this method. This is due to the discontinuity in $x = \frac{\sqrt{2}}{2}$ and $x = 0$ for the respective derivatives of w_1 and w_2. Given that a FEM should approximate a smooth function with good precision, it is expected that a non-smooth function is harder to approximate regardless of step size.

3.4 Refinement Near Singularity

We now want to take a closer look at functions on the $(0,1)$ interval with singularities at $x = 0$. We define the right hand sides,

$$f_1(x) = x^{-\frac{2}{5}} \qquad \text{and} \qquad f_2(x) = x^{-\frac{7}{5}},$$

and observe that $f_1 \in L^2(0,1)$ and $f_2 \notin L^2(0,1)$. We solve the problem (8) with these right hand sides, constants as before, and an equispaced grid, and in figures 4 and 5 we observe that the numerical approximation of especially $f_2(x)$ is quite off. This is due to the singularity that appears at $x = 0$, and to battle this we therefore introduce a new graded grid,

$$x_i = r^{M-i}, \quad i = 1, \dots, M, \quad r \in (0,1),$$

to evaluate more points near the singularity. By introducing this grid, we observe that for $f_2(x)$, the solution with the graded grid is much better. However, for $f_1(x)$, it performs worse than the equispaced one. This is due to the fact that there are no large changes in function values close to $x = 0$ for $f_1(x)$ with the defined constants. This gives the graded grid no advantage, and thus the equispaced grid performs better. With different constants, this is not necessarily the case.

Considering the error tables 1 and 2, we see that the errors reflect the observation. For $f_2(x)$, the graded grid performs better than the equispaced grid in both norms, but the equispaced grid outperforms the graded grid in $f_1(x)$. From table 1 we see that from our tested r's for $f_2(x)$, we observe that $r = 0.8$ is the best choice of r as the error increases again when $r = 0.9$ in both H^1 and L^2 norm. For $f_1(x)$ the error continues to decrease, because the larger r-value makes the graded grid move its first cluster of points further away from $x = 0$.

4 Conclusion

We managed to rewrite our problem on the desired form required by Lax-Milgram, and could therefore approach it knowing that it would obtain an unique solution. The implemented method was diverse, and could be applied to non-smooth solutions with small changes. This is positive, as it means the method can be applied to more intricate problems. However, we observed that even though the problems could be solved to some extent, the errors and convergence rates observed did not coincide with the ones expected for this FEM. This strengthens our knowledge about FEMs, and that they are only really supposed to be applied to smooth solutions.

References

[1] Curry, C. (2018). *TMA4212 Part 2: Introduction to finite element methods.* Available from: Introduction to finite element methods. (Retrieved: 2024/04/07).

[2] Jakobsen, E.R. (2024). Lecture notes week 14. *TMA4212 Numerisk løsning av differensialligninger med differansemetoder.* Available from: Lecture notes week 14. (Retrieved: 2024/04/07).

Appendix

α=1, b=2, c=5
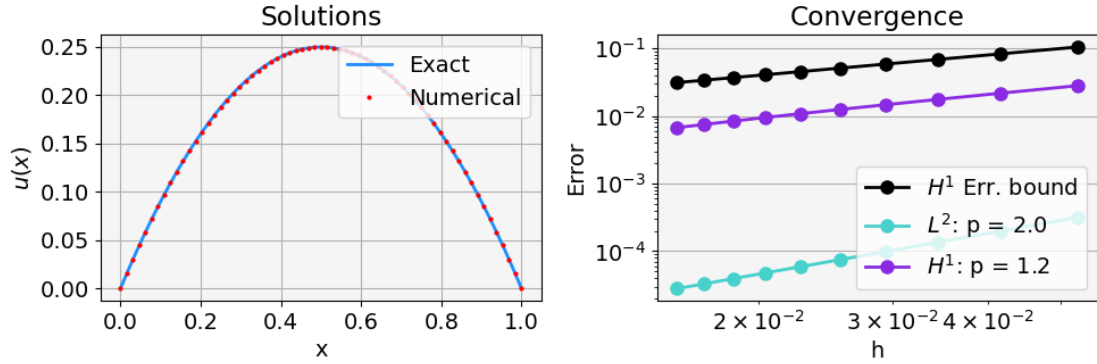

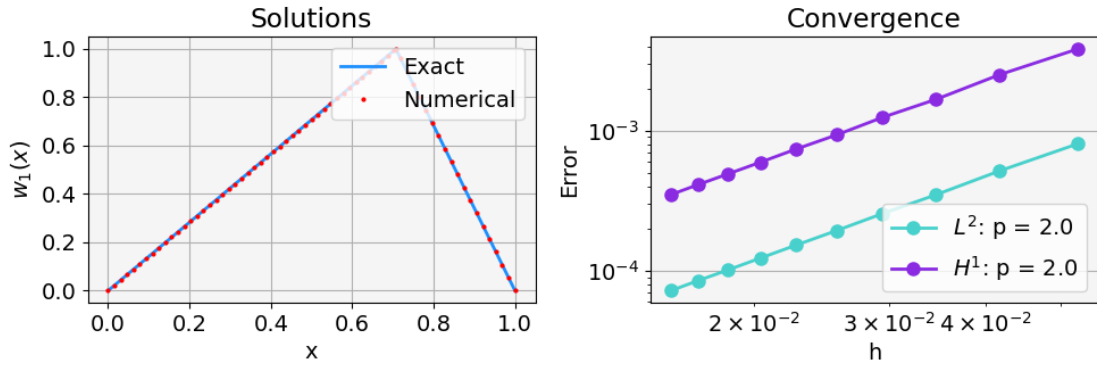Figure 1: Plot of numerical solution and convergence, $u(x) = x(1-x)$

α=1, b=2, c=5

Figure 2: Plot of numerical solution and convergence, $u(x) = w_1(x)$ from (16)
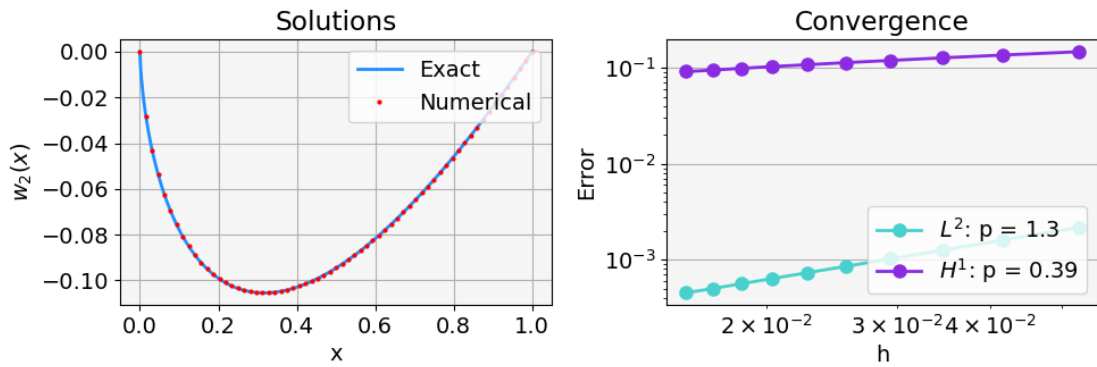
α=1, b=2, c=5

Figure 3: Plot of numerical solution and convergence, $u(x) = w_2(x)$ from (16)
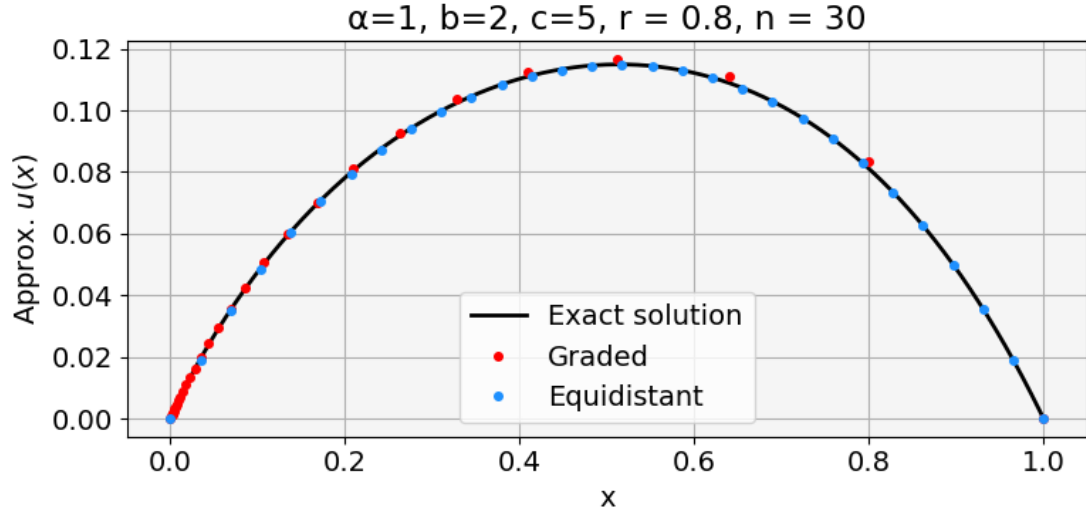
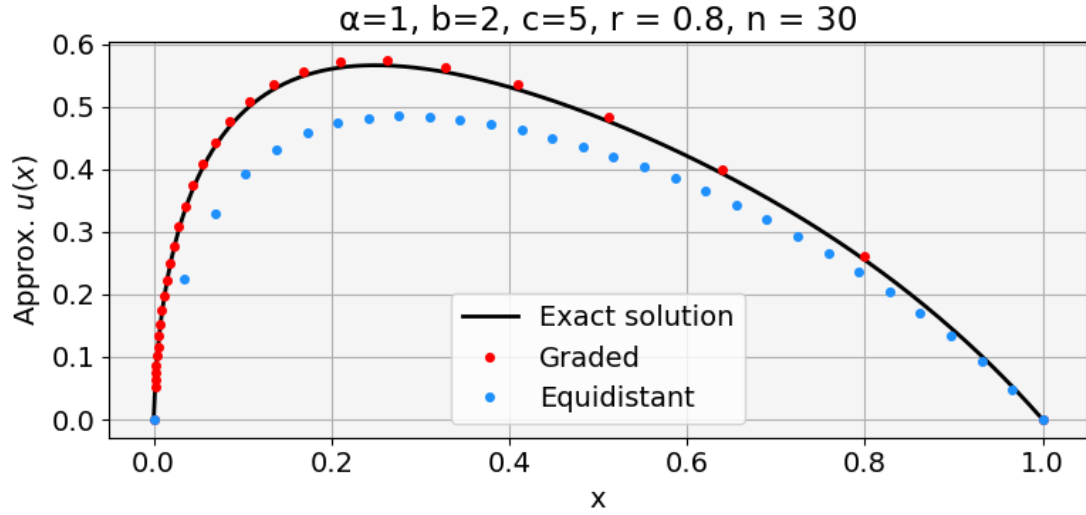Figure 4: Plot of numerical solution, rhs. $f_1(x) = x^{-\frac{2}{5}}$

Figure 5: Plot of numerical solution, rhs. $f_1(x) = x^{-\frac{7}{5}}$

r	$f_1(x)$ Error L^2	$f_1(x)$ Error H^1	$f_2(x)$ Error L^2	$f_2(x)$ Error H^1
0.3	0.02759	0.19010	0.12005	1.27486
0.4	0.02069	0.15631	0.07909	0.95051
0.5	0.01467	0.12677	0.05374	0.76279
0.6	0.00953	0.09944	0.03675	0.63462
0.7	0.00537	0.07298	0.02432	0.52048
0.8	0.00234	0.04695	0.00681	0.11501
0.9	0.00073	0.02440	0.08391	1.50178

Table 1: Errors from refining grid

	n	L^2	H^1
$f_1(x)$	30	0.00038	0.01326
$f_2(x)$	30	0.06517	1.34016

Table 2: Errors from equidistant grids with 30 points